CONF-910478--1

LA-UR 90-3455

Los Alamos National Laboratory is operated by the University of California for the United States Department of Energy under contract W-7405-ENG-36.

LA-UR--90-3455

DE91 002324

TITLE: EXCIMER LASER SURFACE PROCESSING FOR TRIBOLOGICAL APPLICATIONS IN METALS AND CERAMICS

AUTHOR(S): Thomas Roland Jervis
Juha-Pekka Hirvonen
Michael Nastasi

SUBMITTED TO: Society of Tribologists and Lubrication Engineers in the Proceedings of the 1991 Annual Meeting, April 29 - May 2, 1991, Montreal, Canada

Los Alamos National Laboratory
Los Alamos, New Mexico 87545

Excimer Laser Surface Processing for Tribological Applications in Metals and Ceramics

T. R. Jervis, Center for Materials Science,

J-P. Hirvonen, and M. Nastasi, Materials Science and Technology Division

Los Alamos National Laboratory

Los Alamos, NM 87545

ABSTRACT

The use of pulsed excimer lasers, operating at UV wavelengths, for surface modification has many potential applications in the tribology of metals and ceramics. Alterations of surface chemistry and microstructure are possible on standard engineering materials. We have demonstrated improved tribological performance in stainless steel by the formation of a unique oxide and by Ti mixing and in SiC by Ti mixing. Specifically, we have observed reduced friction in dry sliding conditions and a change in the wear process resulting in greatly reduced surface damage. We have also demonstrated the effectiveness of excimer laser mixing in other systems with potential tribological applications.

INTRODUCTION

The use of beam technologies to change the alloy composition and microstructure of the near surface region has been extensively studied in many materials[1-11]. Ion implanted materials are in use in tribological and corrosion applications[13]. The use of CO_2 lasers in industry is widespread for cutting, joining, heat treating, and cladding applications[14]. Excimer lasers, however, are only beginning to make their presence known in industrial applications. This paper will discuss the use of ultra violet (UV) excimer lasers to melt, mix, and/or otherwise change the surface composition and microstructure of materials with specific reference to tribological applications.

The benefits of metastable materials formed by rapid quenching have been explored at great length[15]. However, most techniques for rapid solidification such as melt spinning or splat quenching produce bulk materials. There are other applications, for example tribology or corrosion resistance, in which surface layers could be useful if incorporated into engineering substrates. Laser surface melting and resolidification is a rapid solidification technique useable on practical engineering substrates in a wide variety of material systems. The high quench rate and the fact that the material undergoes a liquid to solid phase change produces a number of effects which can be used in engineering applications. Ion mixing techniques, in which thin films can be mixed together and with the substrate material, also provide high effective quench rates and can be applied to engineering substrates. However, systems for ion implantation are large, expensive and include the need to process in vacuum and in some cases ion beam mixing can be limited by sputtering or formation kinetics[16].

The differences between processing using CO_2 or Nd-YAG lasers in the infrared (IR) and excimer lasers operating in the UV are summarized in Table 1. In the IR, most metals are good reflectors and many ceramics are transparent. In either case, coupling energy from the laser beam to the surface is a problem. In addition, because of the relatively long pulse length, melt depths are much larger, with concomitant changes in surface relief. The essential point is that much more incident laser energy is required to have the same thermal effect as with excimers and the result is a larger *scale* of structural and compositional change. This can be an advantage in some applications (cutting and welding in particular) but processing with a surface relief of 100's or even 10's of microns does not produce a tribologically interesting surface.

Laser	Excimer (KrF)	CO_2 /Nd-YAG
Wavelength	0.248 μm	10.6/1.06 μm
Absorptivity	~ 50%	~ 0.1%
Melt Depth	~ 0.1 μm	~ 100 μm
Melt Duration	~ 100 nsec	~ 100 msec
Cooling Rate	~ 10^{10} K/sec	~ 10^{6} K/sec
Processing Rate	~ 1 cm^2/sec	~ 1 cm^2/sec
Surface Relief	~ 100 nm	~ 10 μm
Power Required	~ 10 W	~ 10 KW

Table 1. Comparison of material processing parameters for UV and IR lasers.

The use of excimer lasers for surface processing can overcome some of the problems inherent in both ion mixing and IR laser technologies. The shallow melt depth and short pulse duration result in negligible surface relief in melted metal systems. Excimer laser processing of polished metal surfaces with an initial surface roughness of ~ 50 nm results in only slight deterioration with a final roughness of ~ 70 nm. Although the melt duration for a single pulse is short, liquid state diffusion can occur to lengths of the order of 5 nm and with multiple pulses mixing and/or segregation over substantial distances is possible. The very high solidification rate may also result in metastable equilibrium phases, a desirable feature in some systems. Because the processing is essentially thermal in nature, the melting is an equilibrium process although the rapid solidification following laser melting may result in non-equilibrium structures. Lasers are relatively cheap and processing requires at most a shield gas, substantially reducing the complexity of the process. Finally, since excimer lasers are comparably efficient to CO_2 lasers in converting electrical to photon energy, substantial energy savings are available for those applications where excimers can replace IR lasers.

COUPLING AND THERMAL EFFECTS

Excimer laser radiation is absorbed within a very short distance in virtually all materials. Typical absorption depths in metals are of the order of 3 nm. Absorption, typically in electron shells, is rapidly thermalized to a heat pulse which is conducted away from the surface. Obviously, there is radiation from the hot surface and convection at the free surface, but these effects are relatively minor at the temperatures and times which of of concern here. The surface of the material melts and the melt front propagates inward until the energy of the pulse is dissipated in the melt process. The melt front then stops and a resolidification front moves back toward the surface. The time history of the temperature of the melted surface layer of metals can be calculated directly from the fundamental optical and thermal constants of the material.

Material	Melt Fluence	Melt Depth	Melt Duration	Cooling Rate
304 SS	0.8 J/cm^2	0.25 μm	20 nsec.	2 x 10^{10} K/sec
Ag	0.8 J/cm^2	0.95 μm	10 nsec.	2 x 10^{10} K/sec
Mo	4.0 J/cm^2	0.40 μm	15 nsec.	5 x 10^{10} K/sec
Be	1.2 J/cm^2	0.60 μm	20 nsec.	2 x 10^{10} K/sec
SiC	1.1 J/cm^2	0.29 μm	15 nsec.	4 x 10^{10} K/sec
ZrO	0.4 J/cm^2	0.15 μm	50 nsec.	1.5 x 10^{10} K/sec

Table 2. Excimer laser melting parameters for various materials. All values refer to fluences just above the melt threshold.

Table 2 gives laser melting parameters as calculated using a simple model of surface melting[17]. It is clear that cooling rate and melt duration are relatively insensitive to material parameters. The principal differences between materials being in melt depth and fluence required to melt. In all cases, the high cooling rates result in the material returning to the initial temperature within 0.01 to 0.1 sec, so that if repetition rates of less than 10 Hz are used, the effect of each pulse is independent. Obviously, if multiple pulses are used, total melt duration increases linearly with the number. Also, if fluences greater than this threshold value are used, greater melt depth and duration are possible, although the use of high fluences can be limited by ablation processes[19].

EXPERIMENTS

We will report here tribological results on three different systems. The oxide formed after many pulses of excimer laser radiation on AISI 304 stainless steel, Ti laser alloyed on AISI 304 stainless steel, and Ti laser alloyed on SiC. In each of these cases, improvements in the tribological properties of the base engineering material were found. In all cases commercially obtained materials were used as substrates with conventional polishing prior to processing. An excimer laser, operating at a wavelength of 248 nm with a pulse length of 25 nsec was used to treat the surface of the material, which was scanned in front of the laser spot. A multi-element refractive beam homogenizer was used to create a uniformly illuminated square spot of approximately 0.25-0.50 cm^2. The scan speed was chosen with different amounts of overlap of each pulse at a repetition rate of 1 Hz so that with each pass, the treated area received several pulses of laser radiation. Thus the amount of processing was varied by varying the number of pulses as well as the incident fluence. In one case, scans were overlapped in both dimensions to further reduce the effect of any remaining beam inhomogeneities. All laser processing was done in room air at a relative humidity (RH) of ~ 40%.

Friction measurements were made using a conventional pin-on-disc apparatus. The pin was a ball 6 mm in diameter. A hardened Cr steel ball was used on the stainless steel substrates and a ruby ball on the SiC substrates. Measurements were carried out in room air without lubrication. Sliding speed was ~ 1.0 cm/sec with a path length ~ 1.0 cm. Loads varied with the substrate but were of the order of the yield stress of the substrate material. The tribological performance of the surfaces was determined by monitoring the friction coefficient as a function of number of cycles and by scanning electron microscope (SEM) examination of the resulting wear track and pin surface.

A. AISI 304 Stainless Steel

Samples of AISI 304 stainless steel approximately 0.3 cm thick were polished to a surface finish of 50 nm (RA). A laser fluence of approximately 1 J-cm^{-2} was used with an overlap of 80% (5 pulses/position). Twenty passes were made, the position was incremented by half the spot dimension perpendicular to the pass direction, and twenty more passes were made etc.. Thus the entire sample received 200 pulses/position with multiple overlap in both dimensions. The resulting film has a transparent gold color. This film has been analyzed extensively[18] and is a spinel oxide of the form $(Fe\text{-}Cr)_3O_4$. Laser processing also transforms the surface martensite induced by the polishing process to austenite.

B. Laser Alloyed Ti/AISI 304 Stainless Steel

A single 100 nm Titanium layer was sputter deposited onto smooth AISI 304 stainless steel substrates. The surface was briefly sputtered before deposition to ensure cleanliness of the surface and to improve the adhesion. Although the samples were kept in a desiccator, no particular effort was made to avoid air exposure after deposition. A laser fluence of the order of 1 $J\text{-}cm^{-2}$ was used with several different overlap settings to probe the effect of the amount of mixing on the properties of the surface. Excimer laser mixing of 50 nm layers on stainless steel has produced an amorphous surface layer with approximately equal Fe and Ti composition after 4 pulses[19].

C. Laser Alloyed Ti/SiC

A single 100 nm layer of Ti was evaporated onto polished polycrystalline SiC substrates using an e-beam evaporation system with a base pressure of the order of 10^{-8} torr.. . The commercially obtained SiC had an initial grain size of about 3.0 μm and contained W as a sintering aid. As above, no extraordinary measures were taken to protect them from oxygen exposure. The samples were processed within one day of evaporation. A fluence of 1.2 $J\text{-}cm^{-2}$ was used with 80% overlap (5 pulses/position). Analysis shows that the surface is a mixed phase material consisting of TiC, TiSi2, and SiC, a mixture consistent with the equilibrium phase diagram[20].

RESULTS AND DISCUSSION

Figure 1 shows the friction history of laser treated and untreated AISI 304 stainless steel at a load of 82 gr. The friction coefficient is dramatically lower, and the torque noise is likewise much lower. SEM micrographs of the disk after 2,500 cycles for the treated and untreated cases are shown in figure 2. The untreated surface shows substantial adhesive wear which is unnoticeable in the treated case. Examination of the pin supports the conclusion that the oxide surface wears steadily but with low friction. There is no evidence of pin wear on the treated surface and no clear evidence for the formation of a well defined transfer film.

Figure 3 shows the results of steady state friction measurements after 1,000 cycles on the Ti alloyed stainless steel surface as a function of number of pulses for a load of 31 gr. As mixing proceeds, a surface layer with optimum composition and structure develops and then, as further diffusion of Fe from the substrate occurs, the friction increases as the surface becomes more Fe rich.

Figure 4 shows the wear track of the Ti alloy layer processed with 9 pulses/position after 1000 passes of the pin at 31 gr load. In the as deposited condition, the wear track in the Ti layer reveals a strong adhesive interaction between the pin and the surface as expected. This interaction is entirely absent after laser processing. The wear track in the alloyed surface is slightly scratched indicating only an abrasive wear mechanism. The absence of deep grooves the track is evidence of increased hardness of the surface after laser processing. It is also of interest to note that the round defect seen in the laser processed sample does not nucleate damage in the wear track. These defects are common artifacts of laser processing, probably due to microscopic inhomogeneities in the surface or local fluctuations in the beam intensity, but are seen in this case not to affect the wear track.

The improved tribological behavior of the surfaces was confirmed by energy dispersive spectroscopy of the pins. In the case of untreated stainless steel, loose wear debris was found on the pin and identified as originating in the stainless steel. Ti was found on pins from the as deposited samples. After testing on laser processed materials, neither loose debris nor Ti deposits were found on the pins in cases where low friction was obtained. Moreover, in these cases the surface of the pin was undamaged and the original surface structure was observable after the friction testing. This is in contrast to the untreated stainless steel and as deposited Ti samples.

Previous work in the Ti-Fe system[21] showed that the greatest improvement in the wear and friction behavior of ion beam processed materials resulted from the formation of a $Ti_{50}Fe_{50}$ amorphous surface layer. We have shown that laser mixing of 50 nm Ti layers with four pulses at a fluence of 1.0 J/cm^2 results in an amorphous alloy with a composition of 40 at% Ti, 40% Fe, 13% Cr and 7% Ni as measured by energy dispersive X-ray spectroscopy. Auger analysis of the layers indicates about 7 at% C in the mixed layer, a value substantially lower than that found in ion implanted or mixed layers, as well as substantial amounts of oxygen[19]. Although we have not analyzed the composition of this particular layer, the results reported here are consistent with all of these results. Because of the cumulative nature of the mixing process, we fully expect that mixing of thicker layers will require more pulses. This effect is seen in Rutherford backscattering spectra of layers of different thickness; it takes a larger number of pulses to obtain equivalent mixing in thicker layers[22].

Figure 5 shows the value of friction measured as a function of number of revolutions for untreated SiC and laser mixed Ti/SiC at a relative humidity (RH) of 50% for a load of 81 gr. Several features are noteworthy. First, the noise in the friction trace, indicated by the error bars in the figure, is dramatically reduced for the surface alloy. This is indicative of a reduction in torque noise and instantaneous forces at the sliding surface. A second feature is the abrupt increase in friction coefficient in the untreated case. Clearly, deterioration of the sliding interface occurs rapidly. In contrast, the alloyed surface exhibits a substantial reduction in initial friction, much lower noise, and a gradual deterioration as the surface is worn through. Although the results shown in the figure are for a single experiment, these features are reproducible.

Figure 6 shows the behavior of this sliding system at a relative humidity of 10%. In each case the load on the pin is the same, 81 gr. The behavior of the ruby-SiC couple actually improves somewhat at lower RH and the ruby-alloy couple deteriorates. This deterioration is seen as a slight increase in initial friction coefficient, an increase in friction noise, and a shorter lifetime.

The contrast in friction behavior is also apparent in the wear mechanism. In the untreated case, the pin is rapidly abraded. The spherical surface is ground flat by sliding against the SiC for 2500 revolutions. Also visible are shear bands at the edge of the worn area indicating high stresses during the sliding process. In contrast, the surface of the ruby pin after similar sliding against the Ti alloyed surface, is undamaged. The key to understanding the wear mechanism is the identification of a transfer film on the pin after sliding on the alloyed disk. Energy dispersive X-ray analysis of the film area confirmed the presence of Ti in this film, indicating that it originates in the disk surface.

Further evidence of a change in the wear mechanism is obtained by examination of the wear track. In figure 7a, a portion of the wear track of the unalloyed disk is shown. The arrow on the figure points to a flake of SiC in the wear track. Numerous cracks and incipient flakes can also be seen. These flakes, and the sharp edges in the disk which result from their removal, contribute to the strongly abrasive wear of the pin. Again in contrast, the entire surface of the laser alloyed wear track is shown in figure 7b. There is no detectable cracking (even when examined at high magnification). Further, the pits seen in the surface, which are artifacts of microscale nonuniformities in the laser surface interaction, do not nucleate damage, even though these surfaces have been exposed to 2500 revolutions and show a friction coefficient comparable to that of the unalloyed surface.

The micrographs in figures 7 were taken on samples measured at a RH of 10%. This choice is deliberate as it represents the worst case for the alloyed material and the best case for the unalloyed SiC. At higher RH, the alloyed surface was even smoother and showed almost no evidence of a wear track. At 50% RH, although the damage to the unalloyed surface was comparable to the low RH case,the friction coefficient surface was higher.

CONCLUSIONS

Because of the stronger coupling of the UV excimer laser light to metal surfaces as compared to more conventional IR techniques, materials processing in the UV holds great promise. We have demonstrated that excimer laser surface processing can have a dramatic effect on the frictional properties of AISI 304 stainless steel, both by the formation of a hard oxide and by the alloying of Ti. We have also shown that similar improvements can be obtained by alloying of ceramics. These three examples demonstrate that excimer laser surface processing is capable of rapidly and efficiently modifying surface microstructure, composition, and chemistry in ways that are beneficial in terms of tribological applications. The modification of engineering alloys whose properties are optimized for structural applications will enable their use in tribological applications The nature of the process allows rapid treatment of large areas with modest investment in equipment and tooling. Obviously, further work will be required to optimize this process for specific applications but the basic principles of modification of the surface chemistry and microstructure have been demonstrated.

ACKNOWLEDGEMENTS

We would like to thank the personnel of the Los Alamos Ion Beam Materials Laboratory for technical assistance. This research was supported by the United States Department of Energy under contract W-7405-ENG-36 by the Los Alamos Center for Materials Science through D. Parkin and by the United States Air Force Wright Aeronautical Laboratory under contract DIO-90-2 through B. D. McConnell.

REFERENCES

1. J. F. Gibbons, L. D. Hess, & T. W. Sigmon, Eds. *Laser and Electron Beam Solid Interactions and Materials Processing,* Mat. Res. Soc. Symp. Proc. **1**, North Holland, Amsterdam, (1981).

2. B. R. Appleton & G. K. Keller, Eds. *Laser and Electron Beam Interactions with Solids,* Mat. Res. Soc. Symp. Proc. **4**, North Holland, Amsterdam, (1982).

3. J. Narayan, W. L. Brown, & R. A. Lemons, Eds. *Laser Solid Interactions and Transient Thermal Processing of Materials,* Mat. Res. Soc. Symp. Proc. **13**, North Holland, Amsterdam, (1983).

4. J. C. C. Fan & N. M. Johnson, Eds. *Energy Beam-Solid Interactions and Transient Thermal Processing,* Mat. Res. Soc. Symp. Proc. **23**, North Holland, Amsterdam, (1984).

5. G. K. Hubler, O. W. Holland, C. R. Clayton, & C. W. White, Eds. *Ion Implantation and Ion Beam Processing of Materials,* Mat. Res. Soc. Symp. Proc. **27**, North Holland, Amsterdam, (1984).

6. D. K. Biegelsen, G. A. Rozgonyi, & C. V. Shank, Eds. *Energy Beam-Solid Interactions and Transient Thermal Processing,* Mat. Res. Soc. Symp. Proc. **35**, Materials Research Society, Pittsburgh, PA, (1985).

7. H. Kurz, G. L. Olson, & J. M. Poate, Eds. *Beam-Solid Interactions and Phase Transformations,* Mat. Res. Soc. Symp. Proc. **51**, Materials Research Society, Pittsburgh, PA, (1986).

8. M. O. Thompson S. T. Picraux, & J. S. Williams, Eds. *Beam-Solid Interactions and Transient Processes,* Mat. Res. Soc. Symp. Proc. **74**, Materials Research Society, Pittsburgh, PA, (1987).

9. M. J. Aziz, L. E. Rehn, & B. Stritzker, Eds. *Fundamentals of Beam-Solid Interactions and Transient Thermal Processing,* Mat. Res. Soc. Symp. Proc. **100**, Materials Research Society, Pittsburgh, PA, (1988).

10. L. E. Rehn, J. Greene, & F. A. Smidt, Eds. *Processing and Characterization of Materials Using Ion Beams,* Mat. Res. Soc. Symp. Proc. **128**, Materials Research Society, Pittsburgh, PA, (1989).

11. S. R. Wilson, R. A. Powell, & D. E. Davies, Eds. *Rapid Thermal Processing of Electronic Materials,* Mat. Res. Soc. Symp. Proc. **92**, Materials Research Society, Pittsburgh, PA, (1987).

12. J. A. Knapp, P. Borgeson, & R. A,. Zuhr, Eds. Beam Solid Interactions: Physical Phenomena, Mat. Res. Soc. Symp. Proc. **157**, Materials Research Society, Pittsburgh, PA, (1990).

13. J. K. Hirvonen, *Ion Implantation in Tribology and Corrosion Science*, J. Vac. Sci. Technol. **15** 1662-1668 (1978).

14. C. W. Draper & P. Mazzoldi, Eds. *Laser Surface Treatment of Metals,* Martinus Nijhoff, Dordrecht, (1986).

15. M. Tenhover, W. L. Johnson, and L. E. Tanner, Eds. *Science and Technology of Rapidly Quenched Alloys,* Mat. Res. Soc. Symp. Proc. **80**, Materials Research Society, Pittsburgh, PA, (1987).

16. J-P. Hirvonen, M. Nastasi, & J. W. Mayer, "Microstructure of Ion-bombarded Fe-Ti and Fe-Ti-C Multilayered Films", J. Appl. Phys. **60** 980 (1986).

17. T. R. Jervis, M. Nastasi, & J-P. Hirvonen, "Formation and modification of surface alloys by excimer laser melting and resolidification" Proc. SPIE **1190** 158 (1990).

18. T. R. Jervis, D. L. Williamson, J-P. Hirvonen, & T. G. Zocco, "Characterization of the Surface Oxide Formed by Excimer Laser Surface Processing of AISI 304 Stainless Steel" Materials Lett. **9** 379 (1990).

19. T. R. Jervis, M. Nastasi, T. G. Zocco, & J. A. Martin, "Formation of Amorphous Ti Alloy Layers by Excimer Laser Mixing of Ti on AISI 304 Stainless Steel" Appl. Phys. Lett. **53** 75 (1988).

20. T. R. Jervis, J-P. Hirvonen, M. Nastasi, and M. R. Cohen, "Laser Mixing of Ti on SiC" Mat. Res. Soc. Symp. Proc. **157** 395 (1990).

21. D. M. Follstaedt, J. A. Knapp, L. E. Pope, F. G. Yost, and S. T. Picraux, "Effects of Ion Implanted C on the Microstructure and Surface Mechanical Properties of Fe Alloys implanted with Ti" Appl. Phys. Lett. **45** 529-531 (1984).

22. T. R. Jervis, M. Nastasi, & T. G. Zocco, "Excimer Laser Mixing of Titanium Layers on AISI 304 Stainless Steel" Mat. Res. Soc. Symp. Proc. **100** 621 (1988).

FIGURE CAPTIONS

1. Friction vs. number of cycles for untreated and excimer laser produced oxide on AISI 304 stainless steel at a load of 82 gr. Error bars give an indication of the magnitude of the torque noise in the measurement.

2. Scanning electron micrograph of the wear tracks of untreated (a) and excimer laser produced oxide (b) on AISI 304 stainless steel after 2,500 cycles at a load of 82 gr.

3. Friction coefficient after 1,000 cycles as a function of number of pulses/position for 100 nm Ti layer on AISI 304 stainless steel.

4. Scanning electron micrograph of wear track of Ti alloyed stainless steel after 1,000 cycles for sample alloyed with 9 pulses/position.

5. Friction coefficient vs. number of cycles for untreated and laser alloyed Ti on SiC at a load of 81 gr and a relative humidity of 50%. Error bars give an indication of the magnitude of the torque noise in the measurement.

6. Friction coefficient vs. number of cycles for untreated and laser alloyed Ti on SiC at a load of 81 gr and a relative humidity of 10%. Error bars give an indication of the magnitude of the torque noise in the measurement.

7. Scanning electron micrograph of the wear tracks of untreated (a) and excimer laser Ti alloy (b) on SIC after 2,500 cycles at a load of 81 gr.

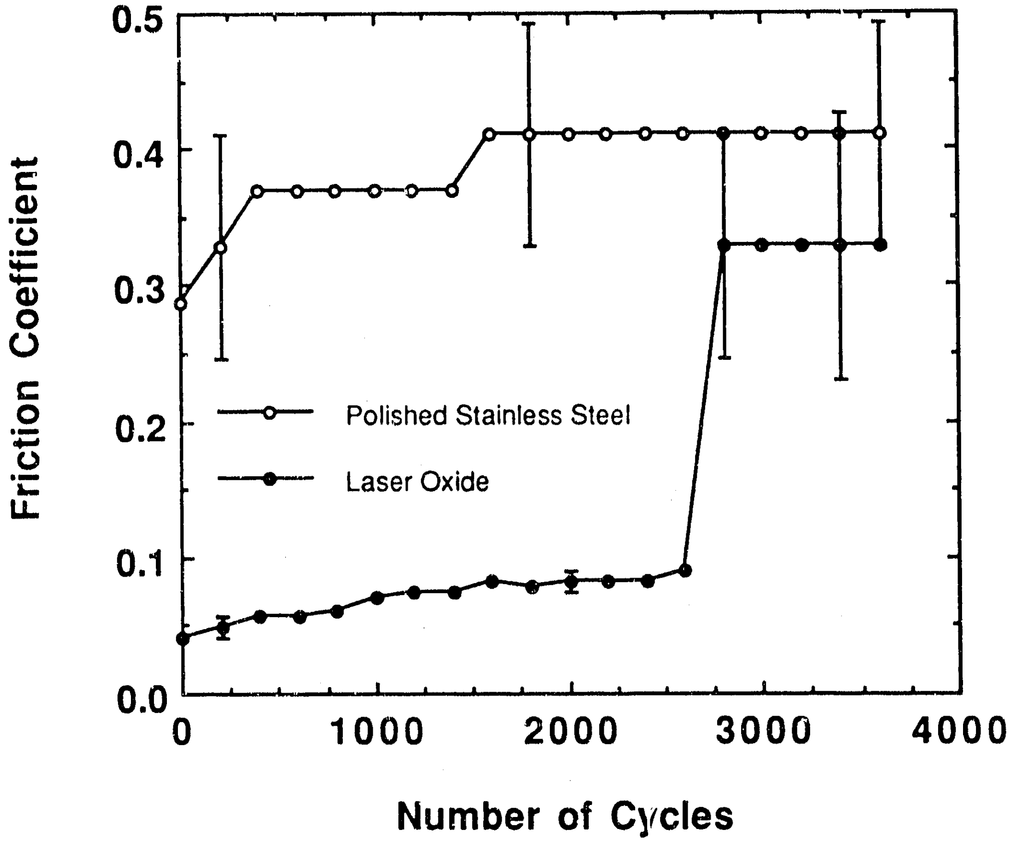

1. Friction vs. number of cycles for untreated and excimer laser produced oxide on AISI 304 stainless steel at a load of 82 gr. Error bars give an indication of the magnitude of the torque noise in the measurement.

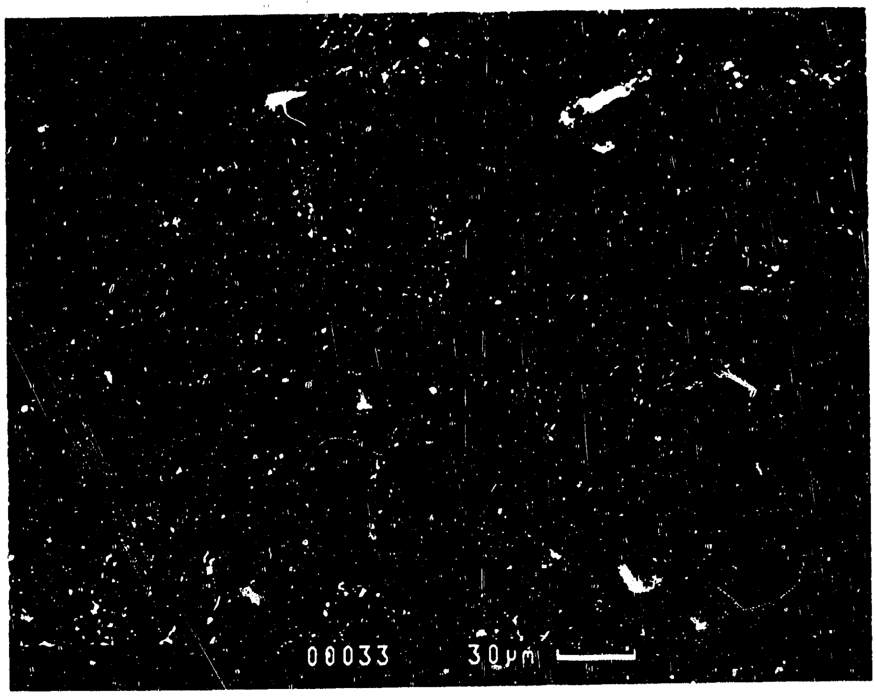

a.

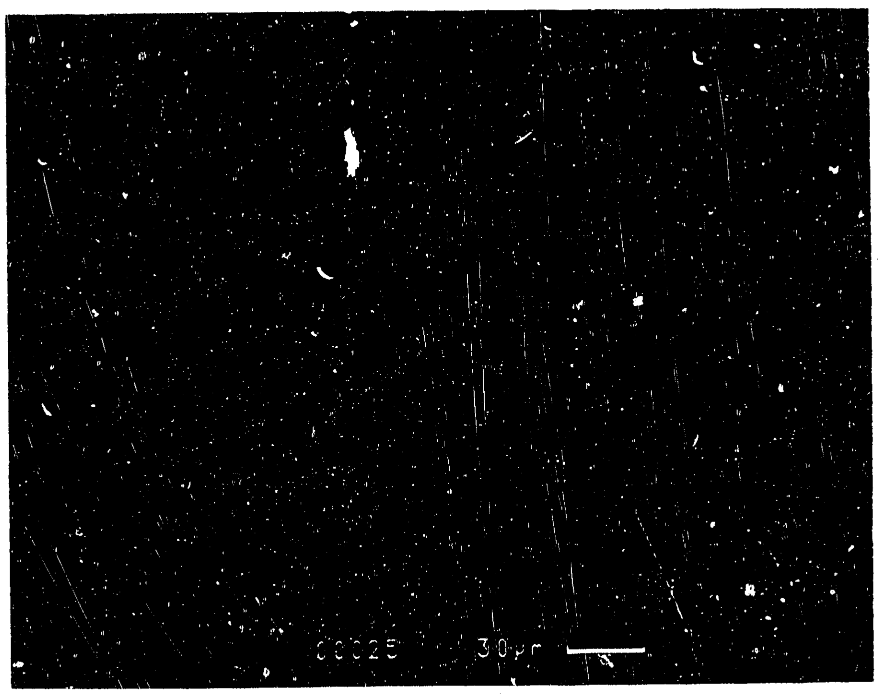

b

2. Scanning electron micrograph of the wear tracks of untreated (a) and excimer laser produced oxide (b) on AISI 304 stainless steel after 2,500 cycles at a load of 82 gr.

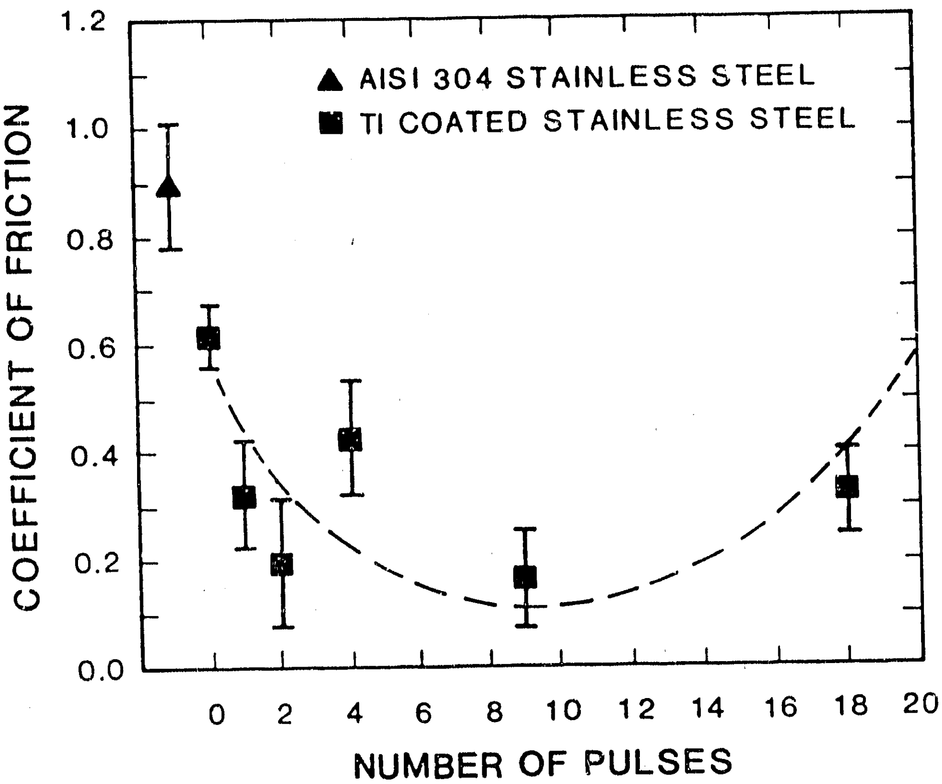

3. Friction coefficient after 1,000 cycles as a function of number of pulses/position for 100 nm Ti layer on AISI 304 stainless steel.

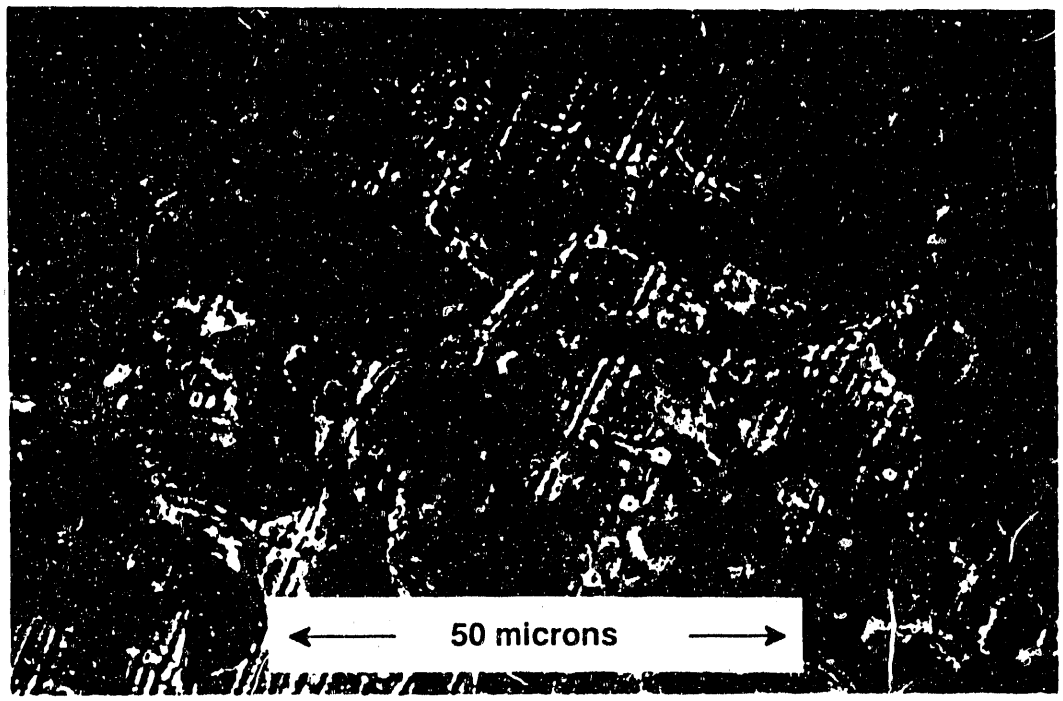

4. Scanning electron micrograph of wear track of Ti alloyed stainless steel after 1,000 cycles for sample alloyed with 9 pulses/position.

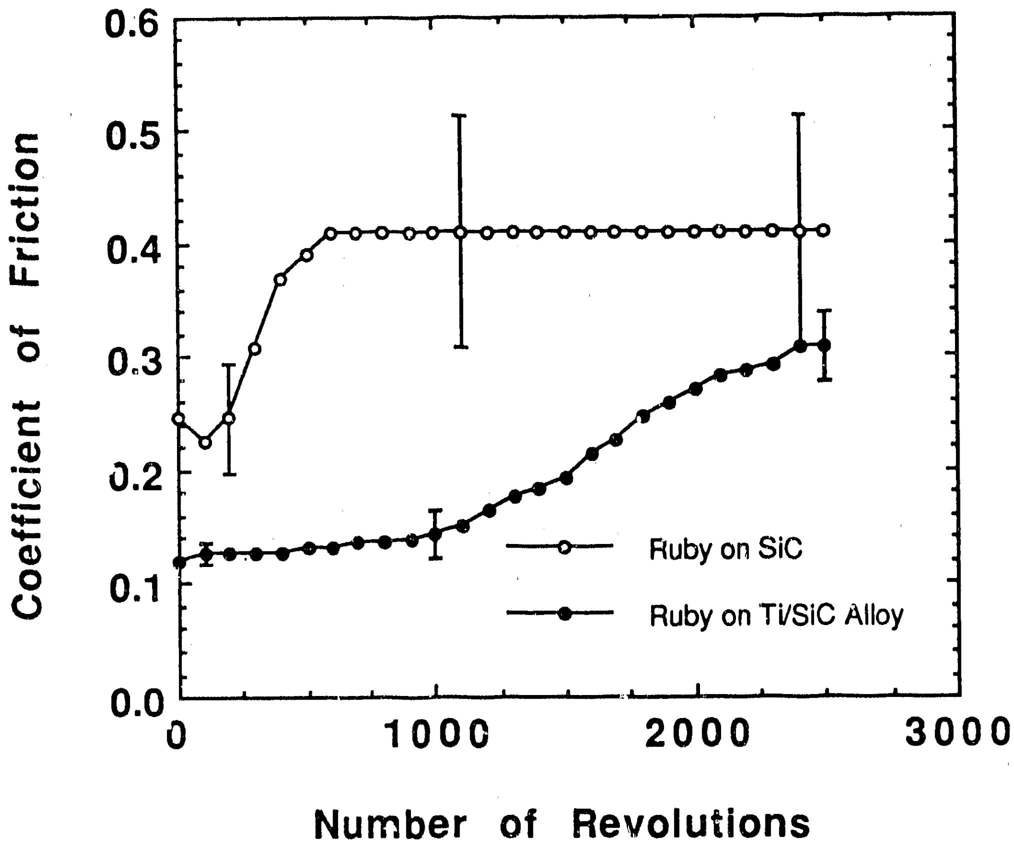

5. Friction coefficient vs. number of cycles for untreated and laser alloyed Ti on SiC at a load of 81 gr and a relative humidity of 50%. Error bars give an indication of the magnitude of the torque noise in the measurement.

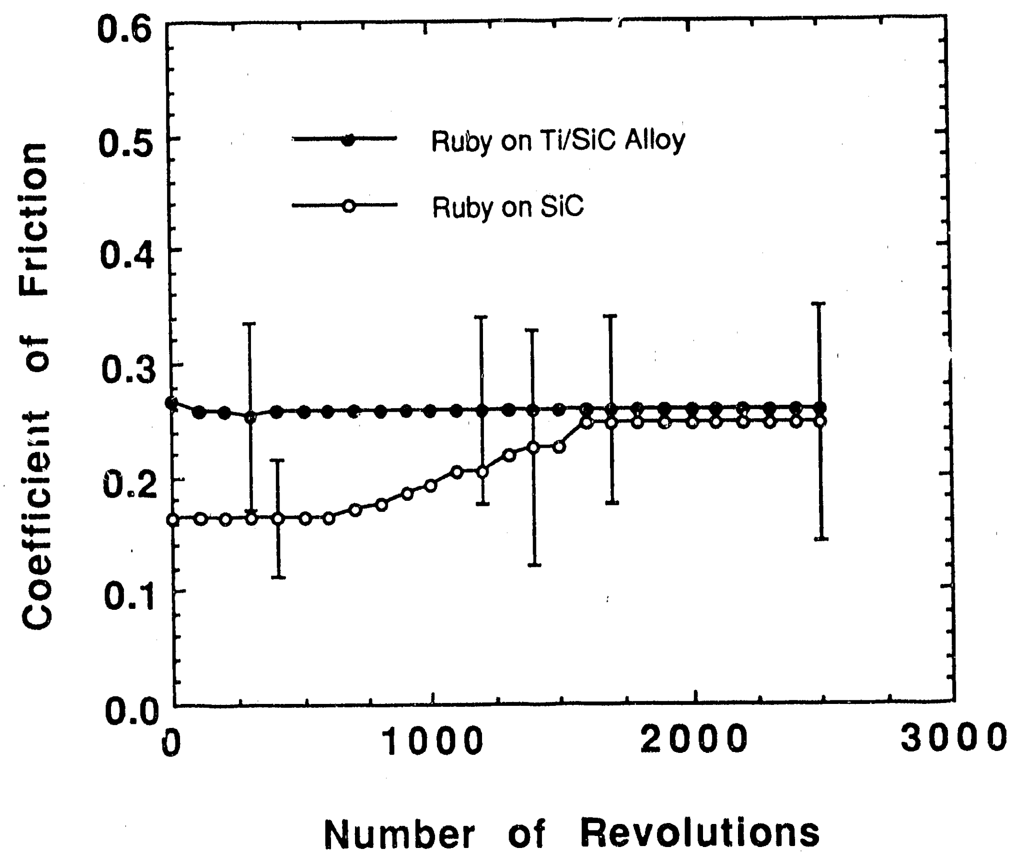

6. Friction coefficient vs. number of cycles for untreated and laser alloyed Ti on SiC at a load of 81 gr and a relative humidity of 10%. Error bars give an indication of the magnitude of the torque noise in the measurement.

←6 μm→

a.

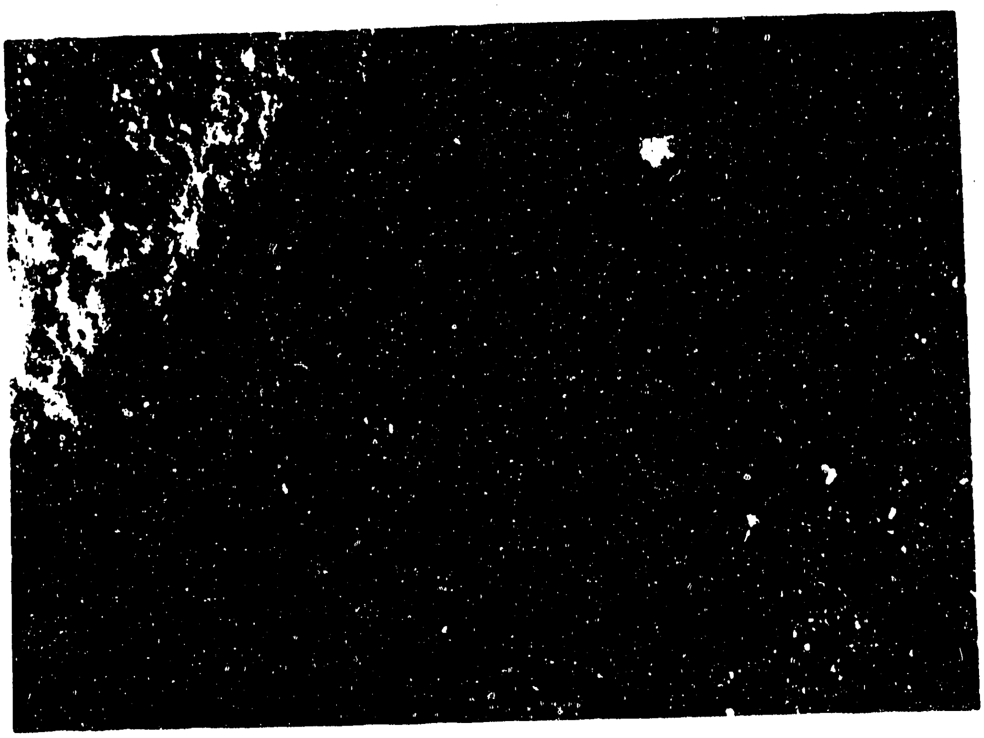

←60 μm→

b.

7. Scanning electron micrograph of the wear tracks of untreated (a) and excimer laser Ti alloy (b) on SIC after 2,500 cycles at a load of 81 gr.

END

DATE FILMED

03 / 06 / 91